Scattering Analysis of Cluster Beams: Formation and Fragmentation of Small Ar_n Clusters

U. Buck and H. Meyer
Max-Planck-Institut für Strömungsforschung, D-3400 Göttingen, Federal Republic of Germany
(Received 22 September 1983)

The formation of Ar_n clusters in a supersonic expansion and their fragmentation by electron impact ionization is measured by analyzing the kinematically different behavior in a scattering experiment. The fragmentation of dimers and trimers is appreciable but depends only slightly on the electron energy.

PACS numbers: 36.40.+d, 35.20.Wg

Since the discovery of cluster formation in supersonic expansions[1] a new area of research has emerged to study the properties and practical applications of these aggregates of atoms and molecules between the gas and the solid phase. The clusters are usually detected by electron impact or photoionization. One of the unsolved problems of this detection mechanism is the unknown fragmentation of the clusters during the ionization process which makes a reliable determination of the neutral cluster distribution in the beam very difficult. There is clear experimental evidence of heavy fragmentation of small clusters studied by means of pure electron impact ionization[2] or in combinations with mass-flux gauge[3] or infrared laser-bolometric techniques,[4] by photoionization,[5] by Penning and heavy-particle impact ionization,[6] and by spectroscopic investigations.[7] Neither effort succeeded in obtaining complete information on the fragmentation process. In this Letter we present an alternative method of getting information on the cluster distribution which exploits the kinematically different behavior in a scattering experiment and which is therefore independent of the detection mechanism. The first reliable information on the fragmentation probability of small Ar clusters is obtained in this way

The principle of the experiment is explained by looking at the kinematic (Newton) diagram of the scattering of Ar_n clusters from He shown in Fig. 1. Because the Ar_n clusters are formed in a supersonic nozzle expansion they have nearly the same velocity but different masses. Therefore, the elastically scattered Ar_n clusters appear according to their different centers of mass at different laboratory scattering angles and different final velocities as marked by the circles in Fig. 1. Because the clusters are heavier than He, there are always two contributions at one laboratory angle, a slow and a fast peak. In addition, each cluster is kinematically constrained to scatter within a certain laboratory angular range, which can be used to distinguish between the lowest two species.[8] However, a combined angular and velocity analysis is necessary in order to separate also the larger clusters from each other.

The experiment has been performed in a crossed molecular beam apparatus which has been described in detail elsewhere.[9,10] The schematic diagram of the apparatus is shown in Fig. 2. The primary cluster beam is produced by expanding Ar through nozzles of 40 to 200 μm in diameter at stagnation pressures from 0.13 to

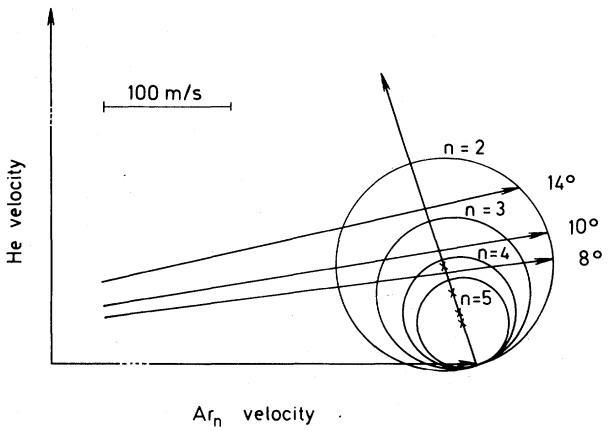

FIG. 1. Newton diagram for the scattering of Ar_n clusters from He for the velocities $v(Ar_n) = 570$ m/s and $v(He) = 1790$ m/s. The different circles denote the positions for final velocities of elastically scattered particles. Note that the velocity arrows are not to scale near the zero point.

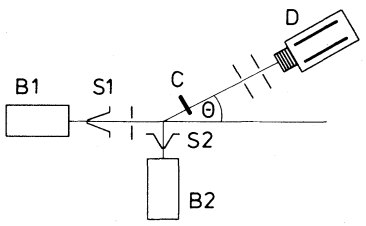

FIG. 2. Schematic diagram of the apparatus. B1, primary beam; B2, secondary beam; S1 and S2, skimmers; C, mechanical pseudorandom chopper; D, detector.

4.00 bars at 300 K. The expansion conditions of the secondary He beam are 30 bars at a nozzle diameter of 30 μm and at 300 K. The velocity distributions of the Ar clusters show the same peak velocity of $v_1 = 570$ m/s with slightly different relative full width at half maximum, $\Delta v/v = 5.2\%$ for the monomer Ar and $\Delta v/v = 4.1\%$ for the dimer Ar_2. The corresponding values for the He beam are $v_2 = 1790$ m/s and $\Delta v/v = 2.3\%$. The two beams are crossed at an intersection angle of 90°. The angular dependence of the scattered beam intensity is measured by rotating the two differentially pumped source chambers relative to the scattering center and the fixed detector unit in the plane of the two crossing beams. The argon clusters are detected by electron impact ionization and mass analyzed by a quadrupole mass filter which is operated in a double differentially pumped detector chamber at pressures lower than 10^{-10} mbar. The final velocity is measured by time-of-flight analysis of the scattered particles with use of the pseudorandom chopping method with a flight path of 449 mm.

The results of measured time-of-flight spectra taken at three different laboratory angles indicated in Fig. 1 at the source pressure $p_0 = 1.4$ bars and a nozzle diameter of $d = 100$ μm are shown in Fig. 3. The scattered Ar_n clusters are detected on the dimer mass (m = 80 u), which we denote $k = 2$, at an electron energy of $E_e = 100$ eV. For each scattering angle the contributions from the different Ar_n clusters are clearly resolved. At $\theta = 14°$ only dimers ($n = 2$) can be detected which is expected according to the Newton diagram of Fig. 1. At $\theta = 10°$ dimers ($n = 2$) and trimers ($n = 3$) are present. In addition, also tetramers ($n = 4$) appear at $\theta = 8°$. Note that in every case the particles are detected on the dimer mass ($k = 2$). The peak width of the final velocity distribution is given by a convolution integral over the angular and velocity distribution of the two beams and the transmission function of the time-of-flight analyzer which accounts for the finite ionization region, the shutter function, and the channel width of the analyzer. A simulation of this distribution function by Monte Carlo techniques using the measured beam and apparatus data and assuming only elastic and weak inelastic scattering is shown in the lower panel of Fig. 3.[11] The comparison indicates that nearly the complete peak width is reproduced. The small amount of intensity left between the two peaks is attributed to dimers resulting from dissociative collisions of higher clusters. Therefore we conclude that the method allows us to get information on the cluster distribution in the beam independent of the detection process. If, in addition, the cluster distribution is measured at different masses we can easily get information on the fragmentation in the ion source. The measured intensity of a peak in the time-of-flight spectrum of the neutral cluster of size n appearing on the mass k times the monomer mass is given by

$$N_{n,k} = \text{const} \times n(\mathrm{Ar}_n; T_0, p_0, d) \times \bar{\sigma}(\mathrm{Ar}_n\text{-He}; g, \theta) f_{n,k}(E_e) C_n(E_e). \quad (1)$$

Besides a constant factor which contains the apparatus functions and the He density, the signal is proportional to (i) the cluster density $n(\mathrm{Ar}_n)$ depending on the source conditions; (ii) the differential cross section for the Ar_n + He scattering at the relative velocity g and the deflection angle θ; (iii) the product of the fragmentation probability $f_{n,k}$ (the fraction of Ar_n appearing on the mass Ar_k) and the ionization probability C_n of Ar_n, both of which essentially depend on the energy E_e

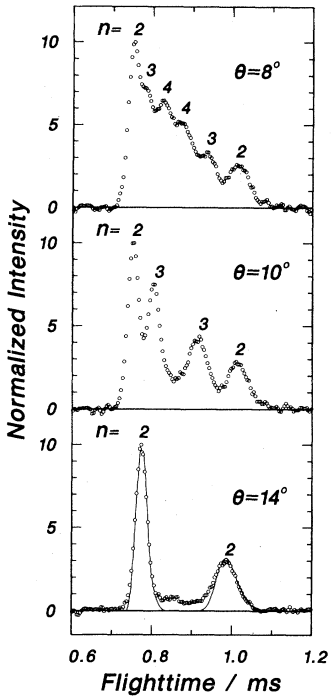

FIG. 3. Measured time-of-flight spectra of Ar_n + He collisions at three different laboratory angles marked in Fig. 1. The clusters of size n are detected on the dimer mass $k = 2$. The solid line in the lower part is calculated with use of the distribution function of the apparatus parameter, averaging, and assuming elastic and weak inelastic (nondissociative) scattering.

of the ionizing electrons.

In a first series of experiments we have measured time-of-flight spectra of Ar trimers and dimers at the monomer, dimer, and trimer masses, $N_{3,i}$ ($i=1,2,3$) and $N_{2,i}$ ($i=1,2$), keeping the source conditions ($p_0=0.92$ bar, $T_0=300$ K, $d=200$ μm) and the scattering angle fixed and varying the electron energy from 30 to 100 eV. In order to normalize the intensities, total differential intensities (without velocity dependence) have also been measured as a function of E_e. Since the conditions for the parent clusters were not changed, the ratio of the peak intensities $N_{n,k}/N_{n,k'}$ directly yields the fragmentation probabilities $f_{n,k}/f_{n,k'}$. Subject to the constraint that $\sum_{k<n} f_{nk}=1$, the f_{nk} values are easily determined. The results are given in Table I. There is appreciable fragmentation of the dimer. Even at low electron energies (30 eV) 50% of the dimers appear on the monomer mass. As a result of increasing electron energy the fragmentation increases slightly. The most striking result concerns neutral trimers. The trimers fragment completely to monomers and dimers. The $f_{3,1}$ value increases with increasing electron energy in a similar way as found for the dimers.

The most important result of the fragmentation study is that the beam contains a large amount of trimers and larger clusters in spite of the fact that no signal on the trimer mass could be detected. Only at high pressures (2 bars at $d=80$ μm) does a small signal appear also on the trimer mass. The investigation of the cluster distribution by means of the differential time-of-flight analysis, however, shows that the corresponding parent clusters are larger than $n=5$. These results clearly show that no stable Ar_3^+ ion formed directly by ionization of Ar_3 exists. A similar behavior has been found in a mass spectrometric study on the unimolecular decomposition of Ar_3^+ at different stagnation gas temperatures.[2] The reason for this behavior[12] is the very stable Ar_2^+ ion with a binding energy of 1.2 eV for the lowest state. During the ionization process a Franck-Condon transition occurs. Since the minimum values of the ion potentials are shifted to smaller values compared to the neutral van der Waals potential, the ion formed is highly vibrationally excited with an excess energy of about 1 eV. With regard to this internal energy the binding energy of Ar_3^+ of about 0.20 eV is small[5,13] and the additional Ar leads to an unstable configuration of the complex. If, on the other hand, an Ar_3^+ ion is detected, it is formed by fragmentation of larger clusters.

TABLE I. Measured fragmentation probabilities $f_{n,k}$ for Ar_n clusters appearing at the Ar_k mass at different electron energies.

E_e (eV)	f_{21}	f_{22}	f_{31}	f_{32}	f_{33}
30	0.50	0.50	0.47	0.53	0.0
40	0.52	0.48	0.52	0.48	0.0
100	0.62	0.38	0.60	0.40	0.0

The implications of these findings are very important, because many experiments on nucleation processes used Ar as a prototype for dimer formation and assumed according to the mass spectrometric detection that no clusters of larger masses are present. This might explain many of the discrepancies in this field.

According to Eq. (1) it is simple to determine ratios of the quantities $n_i \sigma_i C_i / n_j \sigma_j C_j$. They will provide an accurate test for the density, cross-section, and ionization probability ratios, respectively, which can partly be derived from other experiments[14] or calculations. First results show that the ratio C_2/C_1 does not depend very much on the energy E_e of the ionizing electrons if the data are corrected for the fragmentation.

Summarizing the results, the present differential time-of-flight analysis in a scattering experiment allows the unambiguous determination of (1) the fragmentation process of clusters in the ion source and (2) the cluster formation in a supersonic expansion. In the present arrangement clusters up to a maximum size $n=10$ can be resolved. Besides these effects dynamical processes of inelastic and dissociative scattering of clusters can also be studied.

[1]E. W. Becker, K. Bier, and W. Henkes, Z. Phys. 146, 333 (1956).

[2]K. Stephan and T. D. Märk, Chem. Phys. Lett. 90, 51 (1982).

[3]N. Lee and J. B. Fenn, Rev. Sci. Instrum. 49, 1269 (1978).

[4]T. E. Gough and R. E. Miller, Chem. Phys. Lett. 87, 280 (1982).

[5]P. M. Dehmer and S. T. Pratt, J. Chem. Phys. 76, 843 (1982).

[6]H. Haberland, M. Hochwald, R. Waltenspiel, M. Winterer, and D. R. Worsnop, in Proceedings of the Ninth

International Symposium on Molecular Beams, Freiburg, 1983, Book of Extended Abstracts (unpublished), p. 20.

[7]J. Geraedts, S. Setadi, S. Stolte, and J. Reuss, Chem. Phys. Lett. 78, 277 (1981); J. Geraedts, S. Stolte, and J. Reuss, Z. Phys. A 304, 167 (1982).

[8]J. Sibener, R. J. Buss, C. Y. Ng, and Y. T. Lee, Rev. Sci. Instrum. 51, 167 (1980).

[9]U. Buck, F. Huisken, J. Schleusener, and J. Schaefer, J. Chem. Phys. 72, 1512 (1980).

[10]J. Andres, U. Buck, F. Huisken, J. Schleusener, and F. Torello, J. Chem. Phys. 73, 5620 (1980).

[11]In the simulation procedure only inelastic collisions leading to energy transfer less than the dissociation energy have been included. The contribution from inelastic collisions near the dissociation limit never exceeds 10% of the elastic contribution.

[12]See H. Haberland, in *Electronic and Atomic Collisions*, edited by J. Eichler, I. V. Hertel, and N. Stolterfoht, Invited Lectures and Progress Reports of the Thirteenth International Conference on Physics of Electronic and Atomic Collisions, Berlin, 1983 (North-Holland, Amsterdam, 1983), and the references cited therein.

[13]W. R. Wadt, Appl. Phys. Lett. 38, 1030 (1981).

[14]H. P. Godfried and I. F. Silvera, Phys. Rev. A 27, 3019 (1983).